Original Article

Title:

Study of Mechanical Properties of Equine Cortical Bone by Reference Point Indentation Measurement and Finite Element Simulation

Authors:

Kevin Hoffseth[1*], Connor Randall[1], Paul Hansma[2], Henry T. Y. Yang[1]

[1] Department of Mechanical Engineering, University of California Santa Barbara, Santa Barbara, CA 93106, USA
[2] Department of Physics, University of California Santa Barbara, Santa Barbara, CA 93106, USA
* Corresponding author

Corresponding Author Contact Information:

Department of Mechanical Engineering
Engineering Building II, Room 2355
University of California, Santa Barbara
Santa Barbara, CA 93106-5070

(805) 893 5087

kevhoffseth@engineering.ucsb.edu

Keywords:

Cortical Bone; Mechanical Properties; Reference Point Indentation; Finite Elements; Inelastic Deformation

Word Count:

3116

Abstract:

Equine cortical bone properties are studied by Reference Point Indentation utilizing a recently developed instrument, finite element simulation using a Drucker-Prager yield criterion, and conventional mechanical testing. A broad connection is made between the measurement of indentation depth under the dynamic loading of Reference Point Indentation to the cortical bone mechanical properties, especially yield strength and inelastic deformation. It is shown that a Drucker-Prager yield criterion, when calibrated with values from mechanical testing, may be used to model the deformation with accuracy that can be experimentally demonstrated. This suggests an informative link between the ability to measure in-vivo with reference point indentation and traditional ex-vivo measured parameters such as yield strength.

1. Introduction

In large mammals such as humans or horses, bone health is an important topic given the critical role it plays in life. From athletes or racehorses at risk of fracture, to medical professionals investigating the influence of pharmaceuticals, determining the health of bone is of great interest.

Bone is the main load bearing organ of vertebrate animals, making it an important topic of study, and a point of interest since the dawn of modern medicine. Bone can be classified into two main types, cortical (or compact) and trabecular (or spongy). Cortical bone takes the brunt of the forces involved in structural loading, and therefore will be the center of study here.

Cortical bone is a biological hierarchical composite material, with different structural configurations corresponding to different length scales. Bone is easily recognizable in the whole bone form, such as a long bone from a human, or horse, on the meter or sub-meter scale. On the centimeter scale the boundary between cortical and trabecular bone becomes visible. On an even smaller scale, at the sub-millimeter length, the characteristic Haversian, or Osteon system of circular subunits of lamellae enclosing canals filled with blood and nutrients are visible, as seen in Figure 1.

The measurement and testing of cortical bone properties have been researched for decades, with many different approaches. Conventional mechanical testing such as axial loading in tension and compression, and beam bending in three or four-point load setups have been explored extensively (Currey, 2002; Currey, 1999; Burstein et al., 1972; An and Draughn, 2000; Simkin and Robin, 1973; Reilly and Burstein, 1975; Currey, 1990). Various indentation methods have been used as well, ranging from macro scale methods such as Vickers and Rockwell, to using Berkovich indenters with an atomic force microscope or nanoindentor. Most of these tests are performed at quasi-static to low loading rates. Mineral density and chemical composition have been performed extensively as well, with various correlations being made to elastic properties (Mullins et al., 2009; Zhang et al., 2010; Rho et al., 1998; Zysset, 2009; Hoc et al., 2006; Mercer et al., 2006; Tai et al., 2006; Zhang et al., 2008).

One significant complication in testing properties of bone is the question of in- or ex-vivo. Inside a living animal, bone is hydrated and constantly undergoing remodeling and growth. Outside the animal, bone must be kept properly hydrated in order to preserve and/or mimic its natural operating environment. Traditionally, testing of bone in a living patient for diagnosis or treatment is non-trivial, requiring surgery for the removal of bone tissue. This is a large barrier for testing of bone. Overwhelmingly the bone used for the majority of testing, both past and present, is from an animal no longer of the living.

Over the years many investigators have made advances in non-invasive in-vivo testing of bone properties. In particular, x-ray based methods have been extensively developed and are used for testing bone mineral density and tissue composition (Mazess et al., 1990). Another non-invasive technique used is that of ultra-sound measurements, widely studied and generally focused on density and elastic modulus (Jeffcott et al., 1987), but also used to investigate other properties, for example, correlation with failure strength in equine cortical bone (Glade et al., 1986).

Recently, another minimally-invasive in-vivo technique is receiving attention in the medical community, called Reference Point Indentation (RPI) (Bridges et al., 2012; Gallant et al., 2012). A new hand-held reference point indentation instrument, the Osteoprobe, utilizes a rapid, dynamic, indentation, with maximum indentation distance being the primary variable (Randall, 2013). A focus on dynamic indentation is used since most naturally occurring large deformation events occur in bone under impact or rapid loading, such as a sports injury or in a transportation accident. Due to indentation's inherent connection to hardness, pressure and strength, this avenue of testing bone tissue has gained interest as a simple method to test bone quality in a quantitative way. There is growing clinical and laboratory evidence that bone strength can reveal critical information about bone health as a whole, with important implications for fracture risk (Zhang et al., 2010; Rho et al., 1998; Zysset, 2009).

This study will investigate equine cortical bone with the use of reference point indentation, finite element simulation, and simple mechanical testing to determine what mechanical properties are most relevant to maximum indentation depth under rapid dynamic loading, and to what extent a yield criterion such as the one suggested by Drucker-Prager can model inelastic deformation in cortical bone. The integration of multiple investigation methods, illustrated in Figure 2, is used to provide valuable insight into the indentation process by making a connection between indentation depth and conventional mechanical properties.

2. Materials and Methods

2.1 Indentation

Dynamic indentation experiments were carried out on equine cortical bone with a novel, recently developed reference point indentation instrument, the Osteoprobe (Bridges et al., 2012; Randall, 2013). Bone tissue was provided by Purdue University College of Veterinary Medicine, in the form of cross-sections from the third meta-carpal bone. To prepare samples, the periostium and surface tissue were scraped away, then a flat surface, perpendicular to the radial direction (to ensure indentation in the radial direction), was created by cutting, sanding, and polishing, staying within the cortical region. Polishing was performed up to 1500 grit. Samples were hydrated throughout preparation.

For testing, samples were placed under deionized water in a stainless steel vice, and indented normal to the surface, in the radial material direction of the cross section, as seen in Figure 3. Repeated measurements were taken and averaged, with standard deviation calculated.

Two indenter shapes were used to investigate bone behavior, namely a sharp 90° degree cone with a tip radius of order 15 microns versus a blunted 90° degree cone with tip radius of order 35 microns. The shapes share large geometry away from the tip, with a 375 micron major diameter at the top of the cone. Photos and geometry of the tips can be seen in Figure 4. The two tips were chosen to both briefly inspect the effect of tip blunting on cortical bone response, and to verify the ability of the finite element model to predict any differences noted during testing.

In addition to recording the maximum indentation depth, a selected indent site was imaged using a custom atomic force microscope setup with a cantilever built for large depths. This was used for analysis of unloading behavior of the damaged cortical bone.

2.2 Mechanical Testing

Four-point bending and axial compression tests were performed on the cortical bone using an instrumented MTS 810 Universal Test machine. The two different test setups can be seen in Figure 5a and Figure 5b. Material preparation started with the equine third metacarpal cross-sections. Different sample geometries were created for the two different tests, as seen in Figure 5c and 5d. For four-point beam testing, long and thin beams were cut from the cortical region of the cross-section, with the long direction in the cross-sectional (transverse material) plane, perpendicular to the radial material direction. Dimensions ranged from 25.4 - 32.6 mm length, 3.0 - 3.8 mm height, and 4.2 - 5.2 mm width. For axial compression testing, round cylinders with diameters of 6.3 mm and 6.0 – 7.5 mm length were cut out of the cortical region, with cylinder long axis in the radial material direction. Samples were cut same day as testing to prevent undue property degradation, and were kept hydrated throughout preparation and sectioning until test.

The four-point bending test setup used four rollers with custom inner and outer span spacing, restricted by available sample beam dimensions. The axial compression test setup utilized two large platens.

Both crosshead displacement and a laser extensometer were used for test displacement measurement. Two different load cells were used, EATON model 3175-200 for four-point bend testing, and MTS model 661-20A-03 for axial compression testing, with appropriate ranges.

2.3 Finite Element Simulation

In this study, for the sake of simplicity, cortical bone is assumed to be isotropic, and linear elastic, with yield behavior dictated by a linear Drucker-Prager yield criterion. This criterion was chosen in order to accommodate the different yield strengths cortical bone shows under tensile stress or compressive stress, seen in testing and literature (Currey, 2002; Currey, 1999; Burstein et al., 1972). A simple graphical representation of the criterion can be seen in Figure 6. Classical Tresca or Von Mises Criterions often used for metals are unable to account for the unequal strengths and were found to be less than satisfactory in simulating behavior, with Von Mises investigated for comparison here. Parameters for the Drucker-Prager criterion were calculated from test data, with parameters in Table 1. Past the initial yield point, the Drucker Prager criterion is also effectively used as flow criterion, with dilation angle replacing friction angle. A bilinear hardening curve was used, derived from test data values for compressive yield and ultimate strengths.

The indentation simulation was modeled in axisymmetric space, utilizing the assumed material isotropy, with the indenter tip modeled as a rigid body, and the cortical bone as a solid axisymmetric continuum body. The mesh was composed of three node constant strain axisymmetric triangular elements, using 1072 elements, and 593 nodes, total. ABAQUS/Explicit solver was chosen to solve the finite element stiffness equations, due to the fast dynamic nature of the indentation process. Mesh refinement was enhanced around the zone of highest deformation, at the region of contact with the indenter tip. Arbitrary Lagrangian Eulerian (Simulia, 2010) mesh updating was used as a method to treat the high plastic deformation underneath the indenter tip during indentation and ensure elements resist extreme distortion, a possible source of error.

A convergence study was performed numerically with the results of maximum indent depth versus number of nodes shown in Figure 7a. The effect of mesh refinement was studied from very course to very fine, specifically focusing on the finer mesh of a majority of nodes located in the zone under the indenter. Node number was varied from 24 to 1610, with resulting indent depth by sharp indenter tip steady after 291 nodes. It is shown that that the current mesh is sufficiently refined as the convergence is achieved even at the level of 121 nodes, but 480 was used as a conservative compromise with added beneficial resolution. The final mesh used is shown in Figure 7b.

The force profile used in the simulation of the indentation process was composed of two parts. The loading takes the form of a linear increase to a preload of 11N over 0.75 seconds followed directly by a sinusoidal curve of amplitude 40N and half cycle time of 0.0005 seconds. This replicates to an accurate degree the loading characteristics of the reference point indentation instrument used in indentation readings.

3. Results

The results from the mechanical testing showed a large difference in yield strength when comparing four-point bending results and axial compression results. Data can be seen in Table 2. Material yield and failure in four-point bending represents the dominant tensile stress mode on the outer, lower face of the sample beam, while yield and failure in axial compression of the sample cylinder represents compressive stress mode. The difference in behavior has been noticed in previous literature (Currey, 2002; Currey, 1999; Burstein et al., 1972; Reilly and Burstein, 1975), where cortical bone has shown to exhibit different behavior under tensile stress and compressive stress, especially in regards to yielding and inelasticity.

Figure 8 displays two of the different experimental stress strain curves of cortical bone, one from four-point bending and one from axial compression. It is evident that there is a large difference in behavior between tensile stress and compressive stress, as is visible in Figure 8c. In tension, it was observed that cortical bone fails early due to Mode 1 fracture, usually after a small amount of post yield plastic deformation. In contrast, while under compression, along with avoidance of Mode 1 cracking, a much larger amount of plasticity is available. The ratio of compressive yield/tensile yield strengths in previous studies has been shown to vary around 1.5 to 1.7 (Currey, 2002; Currey, 1999; Burstein et al., 1972). In this study it was found to be 1.85 using the compressive yield stress found from axial compression test data, and tensile yield stress found from four-point bending test data. The somewhat larger value could be due to the material orientation during beam testing, some undetected cracking and flaws from preparation causing premature failure, or a result of undetected illness in the equine donor health.

Variation in testing was similar to that expected of biological composites. Both steel rollers and nylon 6/6 rollers were used in four-point beam testing, with the Nylon 6/6 rollers used in hopes of alleviating stress concentrations in the beams under load. Their use showed a lesser Young's Modulus, but appeared to slightly aid in capturing yield strength and failure.

The results of simulating dynamic equine cortical bone indentation using a Drucker-Prager Yield Criterion with material parameters determined from mechanical testing were promising. Results from both a Drucker-Prager Yield Criterion and a Von Mises Yield Criterion for the sharp tip indenter can be seen in Table 3. Both criterions used the same material parameters determined from mechanical testing, except for the ability of Drucker-Prager to handle different yield strengths under tensile stress or compressive stress, and also pressure dependence. The Von Mises Yield Criterion used a single yield strength that was the average of the tensile yield strength and compressive yield strength found in testing. The Drucker-Prager Yield Criterion appears more accurate at replicating experimental values, being less than 8% off. The use of the Von Mises Yield Criterion results in value double that of experiment. The discrepancy is large and shows the suitability of the Drucker-Prager Yield Criterion in simulating the cortical bone response.

Simulation results compared to investigation by atomic force microscope (AFM) are shown in Figure 9, along with a simulation mesh contour showing values of plastic equivalent strain (PEEQ). Cortical bone seems to display a surprising amount of plastic deformation under indentation, and use of the Drucker-Prager Yield Criterion results in high values of plastic strain, with the immediate region under the indenter tip exceeding 2, seen in Figure 9a. While the stresses involved in indentation are not solely compressive, the ability to deform without catastrophic fracture and with only light cracking show a degree of plasticity reminiscent of the compressive behavior seen in testing, contrary to that of weak tensile failure in fracture. The use of a plasticity based model to simulate the deformation response at high plastic strain has shown to mimic to good effect the response of bone under rapid indentation, and indeed, the resulting residual indent geometry in the finite element model is very similar to that of the real cortical bone, shown in AFM profile for comparison. Both Figure 9c and Figure 9d display the finite element simulation results of unloading in comparison to the AFM profile. In order to accommodate possible damage of the bone during the loading process, two different approaches were used to study the unloading regime and residual indent; one utilized a constant elastic modulus throughout the entire simulation, seen in Figure 9c; while the second reduced the elastic modulus to reflect deformation and damage in the bone, which is seen in Figure 9d.   Exploration of degradation of elastic modulus due to damage can be seen in (Pattin et al., 1996).

Figure 10 displays the favorable comparison of simulation and experimental results for both sharp and blunt tip geometry, using the same loading. Both simulations show close agreement, here demonstrating the accuracy of the Drucker-Prager Yield Criterion in replicating the deformation behavior in cortical bone across disparate indenter geometry. Of minor note is that the blunt tip results may be more accurate than the sharp tip, possibly due to difficulties in numerically meshing extremely sharp geometries.

4. Discussion

Equine Cortical bone has been studied by reference point indentation, conventional mechanical testing, and finite element simulation. Results have shown that the use of a linear Drucker-Prager Yield Criterion is successful at modeling the dynamic indentation response of cortical bone on the micro-structural osteon level, with direct connection to testable mechanical properties, namely the tensile and compressive yield strengths, and elastic modulus. With all experiments being performed on the same donor material, we can be confident in validation of the approach taken. Consideration of the rapid load rate (~80000 N/s in the impact stage) shows suitability for understanding damage and response in a load regime with direct relation to animal injuries from fall or impact, for instance in a race or accident. The simplicity of use of the reference point indentation method, with its ability to test in-vivo, and the demonstrated link of indentation depth to yield strength could prove beneficial for testing or diagnostics in a medical setting, and an important first step towards connecting indentation response to fracture risk in a mechanistic way.

These results show the practical benefit of viewing the inelastic post yield behavior as a type of plasticity, or pseudo-plasticity, although we must not gloss over the fracture mechanisms most certainly occurring at the small scale during this idealized plasticity, probably in the form of micro cracking (Gallant et al., 2012; Ritchie et al., 2009) or a few larger cracks initiating (Ritchie et al., 2009). However, even with these processes taking place, the idealization of the dynamic indent deformation as a plastic process with behavior modeled by Drucker-Prager Yield Criterion shows to be useful in studying the connection between dynamic indent depth and mechanical properties of cortical bone. Furthermore, the ability to replicate difference in indentation depth due to tip geometry is an initial validation of the general suitability of the model in simulation of cortical bone deformation and inelasticity.

Further study is needed in some areas, most obviously that of incorporating some degree of fracture into the model. Fracture is a significant deformation mechanism in bone at large length scales, and to what extent it is contributing under indentation on the osteonal level remains a question. Bone material from more than one donor would be invaluable as well, as it would help in validation of the strength-indent depth connections. Last, determining the effect of health of the donor animal on the plastic response would be important to investigate.

The next step, once further study is made, would be to analyze the difference in response of single donor material after introducing artificial damage, of various types. Using the same integrated research approach, the influence of various factors and mechanisms of the cortical bone under the different loading types could be examined, with obvious benefits to knowledge of cortical bone fracture risk, age effects on mechanical properties, and long term pharmaceutical effects, among others.

Conflict of Interest

Paul Hansma is a member of Active Life Scientific, which sells the Biodent product line of Reference Point Indentation instruments for research use only.

Acknowledgements

The authors would like to gratefully acknowledge funding by NSF through grant CMMI-1031244, and by NIH through grant RO1 GM055354. Additionally, the authors would like to acknowledge the support of the UC Santa Barbara Physics Department, and also thank Dr. Srinivasan Chandrasekar, of the Department of Industrial Engineering, Purdue University, for thoughtful guidance and discussion.

References

An, Y.H, Draughn, R.A., 2000. Mechanical testing of bone and the bone-implant interface, CRC Press, Boca Raton, FL.

Bridges, D., Randall, C., Hansma, P.K., 2012, "A new device for performing reference point indentation without a reference probe," Review of Scientific Instruments 83, 044301-044301-8.

Burstein, A.H., Currey, J.D., Frankel, V.H., Reilly, D.T., 1972. The ultimate properties of bone tissue: the effects of yielding. Journal of Biomechanics 5, 35-44.

Currey, J.D., 1990. Physical characteristics affecting the tensile failure properties of compact bone. Journal of Biomechanics 8, 837-844.

Currey, J.D., 1999. What determines the bending strength of compact bone? Journal of Experimental Biology 202, 2495-2503.

Currey, J.D., 2002. Bones: Structure and Mechanics. Princeton University Press, Princeton, NJ.

Gallant, Maxime A., Drew M. Brown, Jason M. Organ, Matthew R. Allen, and David B. Burr, 2012. Reference-point indentation correlates with bone toughness assessed using whole-bone traditional mechanical testing. Bone 53, 301-305.

Glade, M.J., Luba, N.K., Schryver, H.F., 1986. Effects of age and diet on the development of mechanical strength by the third metacarpal and metatarsal bones of young horses. Journal of Animal Science 63, 1432-1444.

Hoc, T., Henry, L., Verdier, M., Aubry, D., Sedel, L., Meunier, A., 2006. Effect of microstructure on the mechanical properties of Haversian cortical bone. Bone 38, 466-474.

Jeffcott, L. B., S. H. W. Buckingham, and R. N. McCartney, 1987. Noninvasive measurement of bone quality in horses and changes associated with exercise. Equine Exercise Physiology 2, 615-630.

Mazess, Richard B., et al., 1990. Dual-energy x-ray absorptiometry for total-body and regional bone-mineral and soft-tissue composition. The American Journal of Clinical Nutrition 51, 1106-1112.

Mercer, C., He, M.Y., Wang, R., Evans, A.G., 2006. Mechanisms governing the inelastic deformation of cortical bone and application to trabecular bone. Acta Biomaterialia 2, 59-68.

Mullins, L.P., Bruzzi, M.S., McHugh, P.E., 2009. Calibration of a constitutive model for the post-yield behavior of cortical bone. Journal of the Mechanical Behavior of Biomedical Materials 2, 460-470.

Reilly, D.T., Burstein, A.H., 1975. The elastic and ultimate properties of compact bone tissue. Journal of Biomechanics 8, 394-405.

Pattin, C. A., W. E. Caler, and D. R. Carter, 1996. Cyclic mechanical property degradation during fatigue loading of cortical bone. Journal of Biomechanics 29, 69-79.

Randall C., Bridges D., Guerri R., et al., 2013. Applications of a new hand-held reference point indentation instrument measuring bone material strength. Journal of Medical Devices (Epub ahead of print 7 May 2013).

Rho, J.Y., Kuhn-Spearing, L., Zioupos, P., 1998. Mechanical Properties and the hierarchical structure of bone. Medical Engineering & Physics 20, 92-102.

Ritchie, Robert O., Markus J. Buehler, and Paul Hansma, 2009. Plasticity and toughness in bone. Physics Today 62, 41-47.

Simkin, A., Robin, G., 1973. The Mechanical Testing of Bone in Bending. Journal of Biomechanics 6, 31-39.

Simulia, 2010*,* ABAQUS 6.10 User Documentation.

Tai, K., Ulm, F.J., Ortiz, C., 2006. Nanogranular Origins of the Strength of Bone. Nano Letters, 6, 2520-2525.

Zhang, J., Niebur, G.L., Ovaert, T.C., 2008. Mechanical property determination of bone through nano- and micro-indentation testing and finite element simulation. Journal of Biomechanics, 41, 267-275.

Zhang, J., Michalenko, M.M., Kuhl, E., Ovaert, T.C., 2010. Characterization of indentation response and stiffness reduction of bone using a continuum damage model. Journal of the Mechanical Behavior of Biomedical Materials 3, 189-202.

Zysset, P.K., 2009. Indentation of bone tissue: a short review. Osteoporosis International 20, 1049-1055.

Tables

Table 1. Drucker-Prager parameter values calculated with mechanical test data.

Linear Drucker-Prager Parameters		
β	K	Φ
32.1	0.827	10

Table 2. Mechanical Testing Results, showing average values with standard deviation in parentheses.

Test Type	Young's Modulus (GPa)	Yield Strength (MPa)	Ultimate Strength (MPa)
Axial Compression (N=4)	2.45 (0.98)	89.15 (5.92)	103.37 (12.80)
Four-point Bending (N=5, Nylon rollers)	5.59 (0.89)	48.37 (2.95)	52.90 (3.81)
Four-point Bending (N=5, Steel rollers)	7.16 (1.72)	34.85 (4.17)	42.08 (4.17)

Table 3. Indentation values of experiment versus selected yield criterion.

	Experiment	Drucker-Prager	Von Mises
Depth	159.20	147.1	315.2

Figures

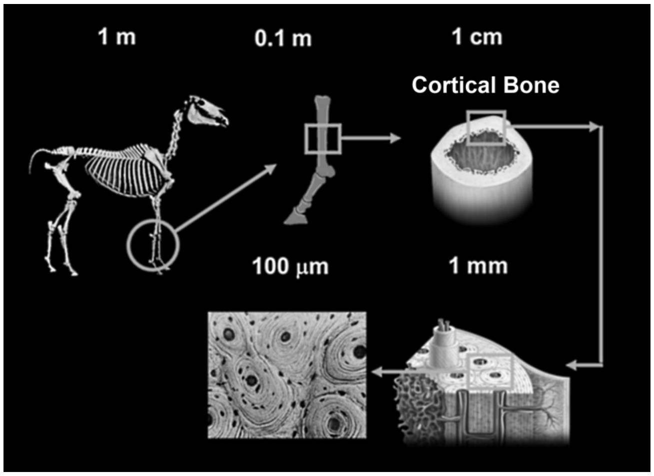

Fig. 1. Description of the hierarchical structural configuration of bone at critical length scales.

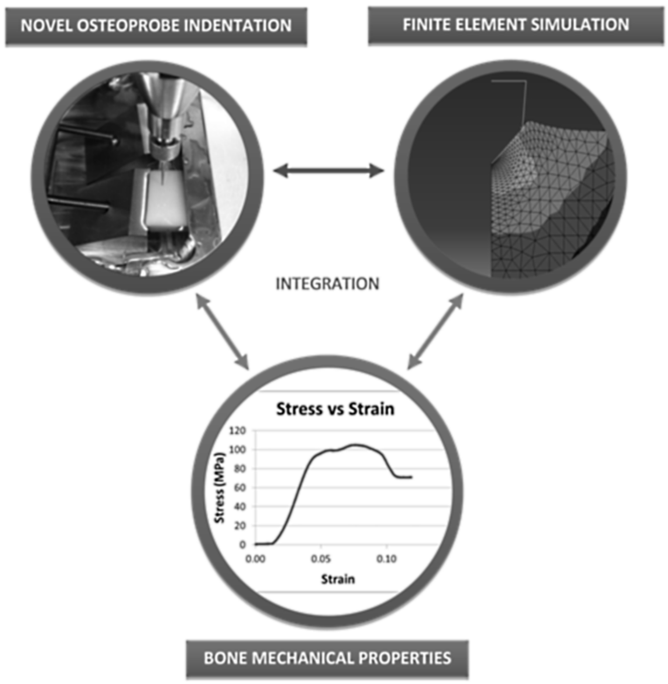

Fig. 2. Integrating a rapid in-vivo handheld indentation of cortical bone and finite element simulations on indentation response and bone mechanical properties.

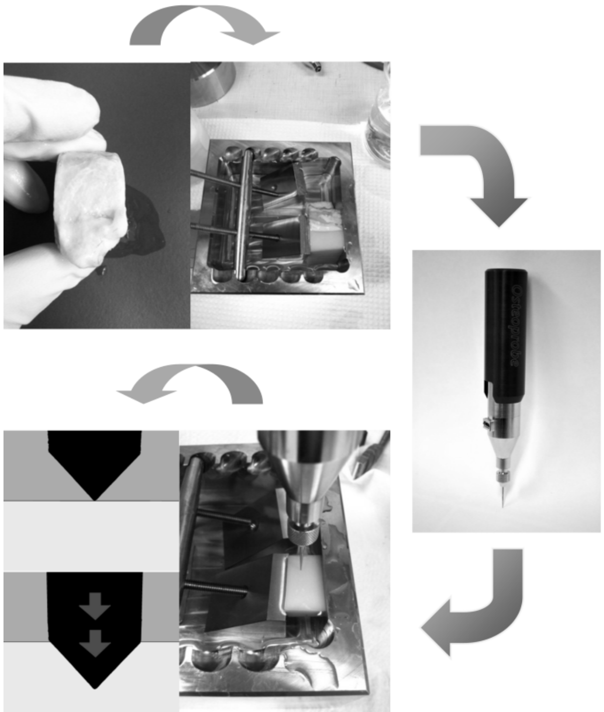

Fig. 3. The process of indentation of the equine third metacarpal. The specimen is fixed in a clamp under solution, then indented with the Osteoprobe.

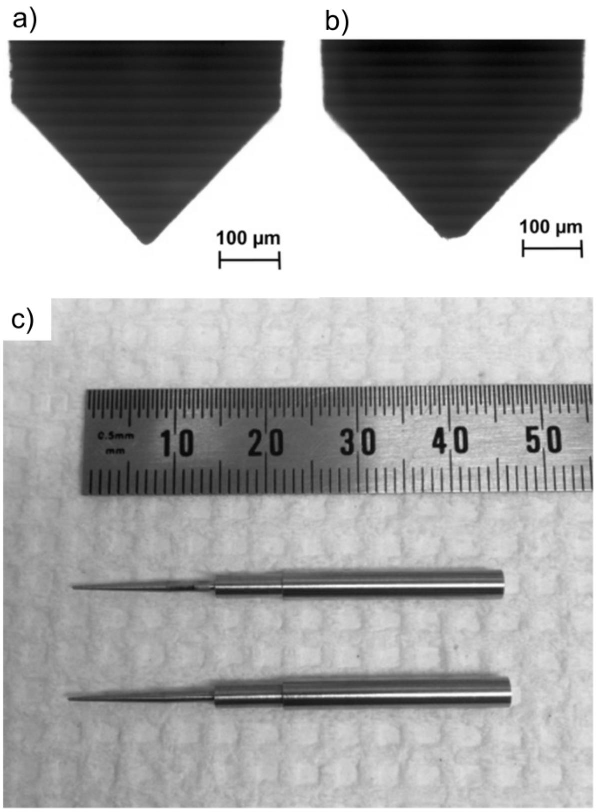

Fig. 4. Photos of indenter shapes as taken through optical microscope, used in experiment with a) sharp tip of radius < 15 microns, and b) blunt tip radius of ≈35 microns. Macro scale is shown in c).

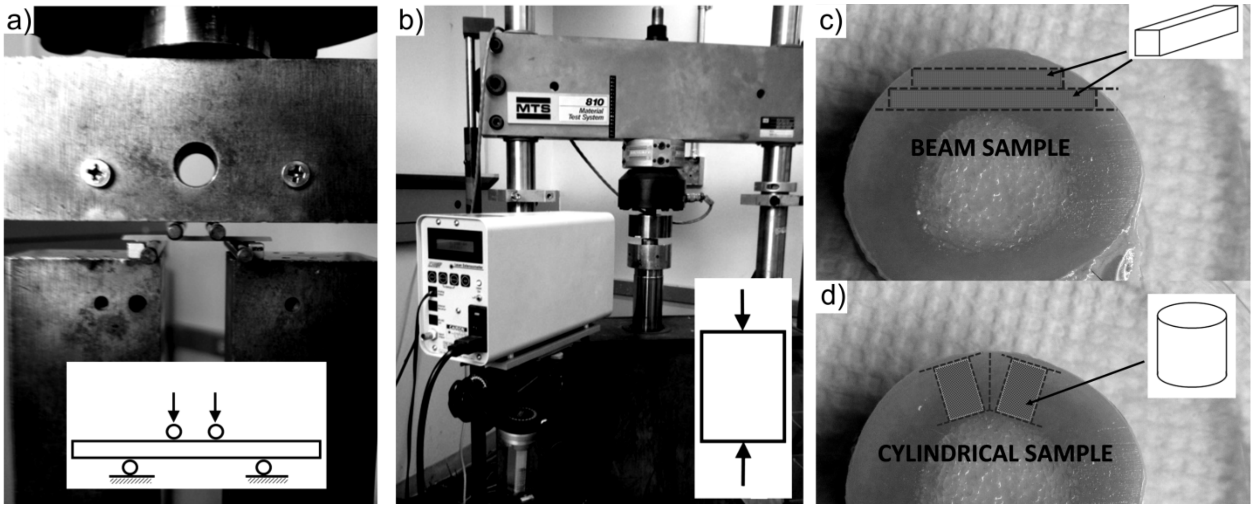

Fig. 5. Test setups for a) four-point bend testing and b) compression testing, used for determining cortical bone mechanical properties. Test specimen sectioning shown for c) beams and d) circular columns.

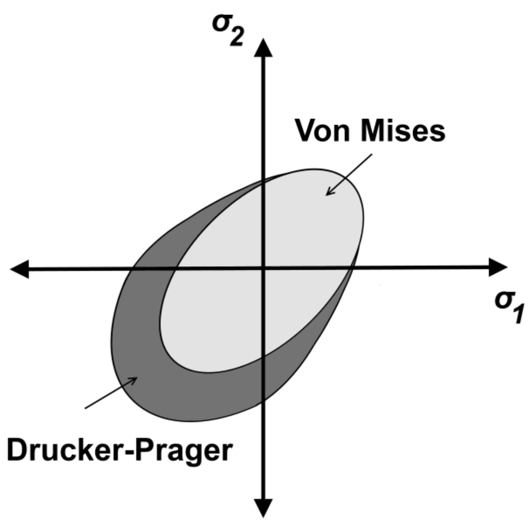

Fig. 6. Visual depiction of the difference between Linear Drucker-Prager and Von Mises yield criterions in the principal σ1-σ2 plane.

a)

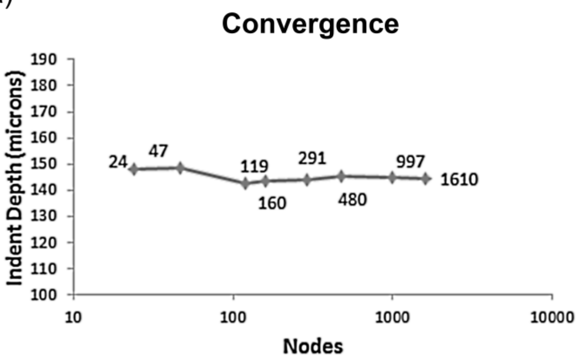

b)

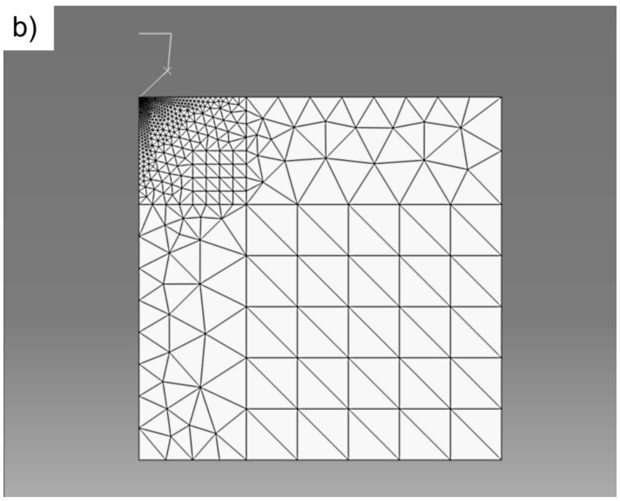

Fig. 7. Shown in a) is effect of mesh refinement of the triangular shaped zone immediately underneath the indenter geometry on the convergence of indent results, with b) displaying the mesh used for indent simulation.

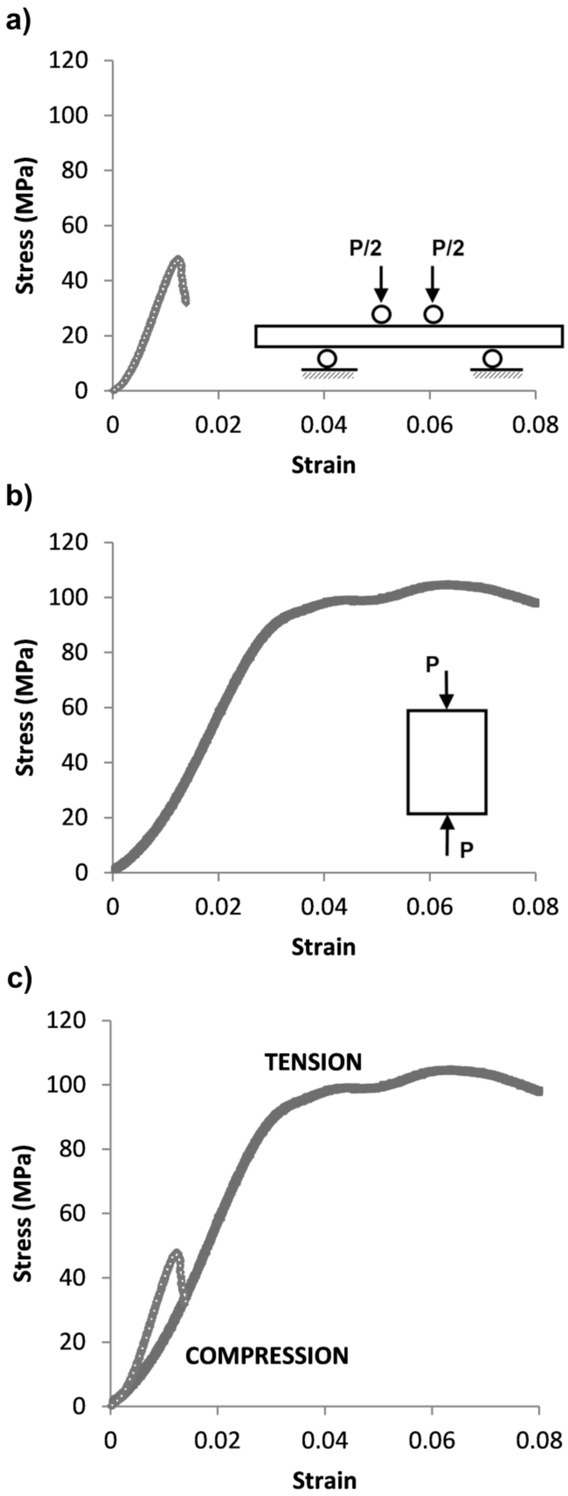

Fig. 8. Example stress-strain curves of cortical bone from mechanical testing, with a) tensile stress in bending; b) compressive stress in axial compression; c) comparison showing the stark difference in behavior.

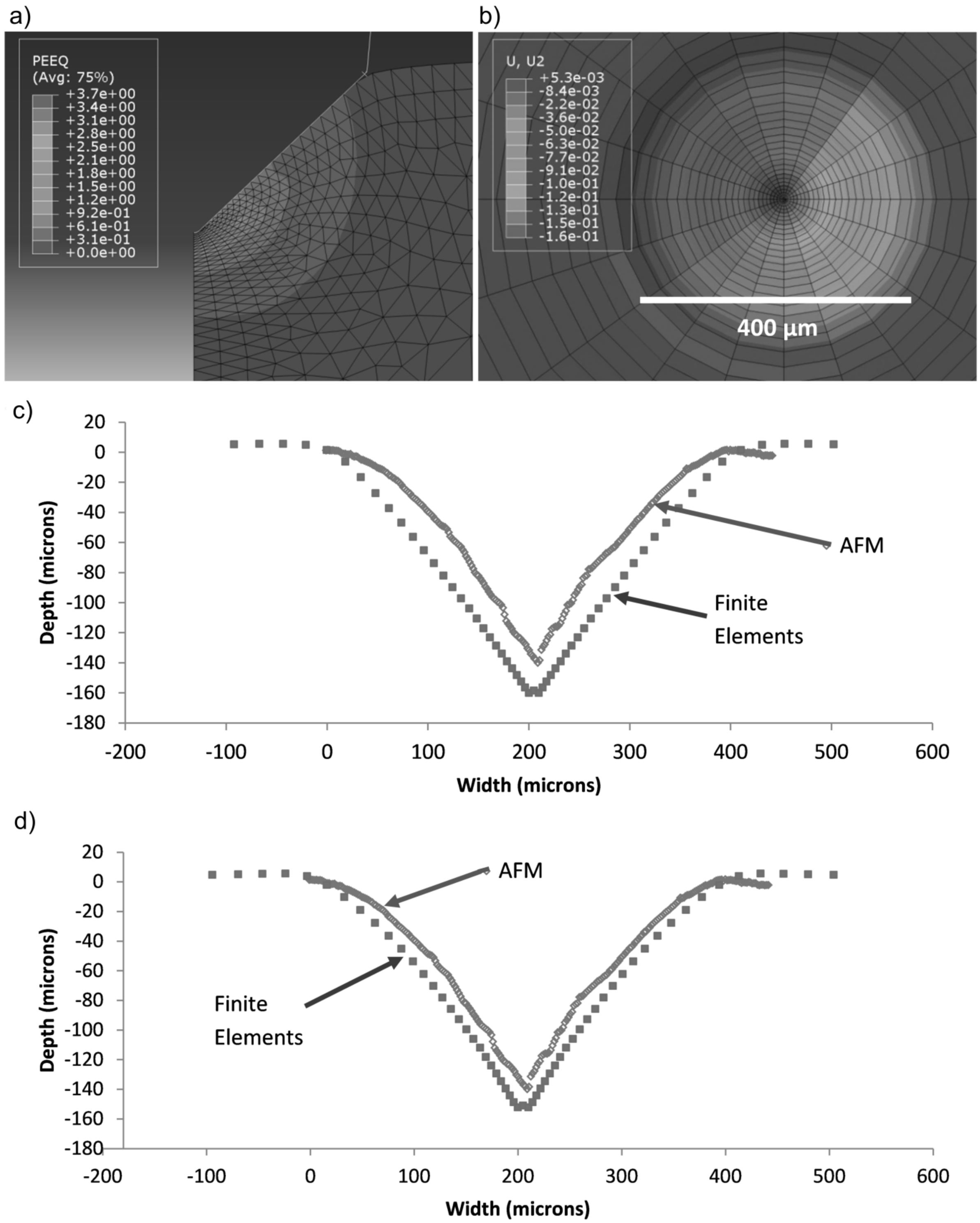

Fig. 9. Results of sharp cone indent simulation, showing a) effective plastic strain at maximum indent depth; b) overhead view of resulting indentation; c) comparing finite element simulation and AFM line scan with constant elastic modulus; d) comparison with simulation using elastic modulus reduction throughout loading as to mimic damage.

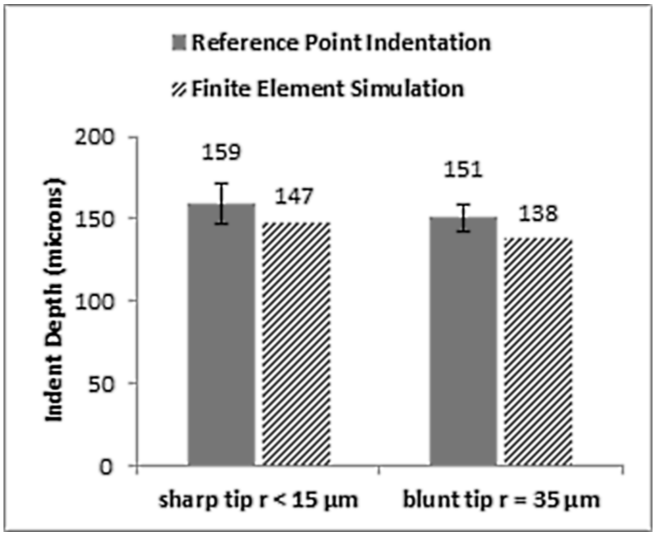

Fig. 10. Comparison of reference point indentation and finite element simulation results for indentation of equine cortical bone with both sharp and blunt tip indenter geometries. Black error bars show standard deviation of reference point indentation readings.